Microhand With Internal Visual System

Wook Choi, Minoo Akbarian, Vladimir Rubtsov, and Chang-Jin "CJ" Kim, *Member, IEEE*

***Abstract*—A pneumatically operated four-fingered micromanipulator (a "microhand") with a fiber-based internal visual system is developed using microelectromechanical systems fabrication techniques. This "seeing" microhand transfers images generated by the optical system equipped at the palm of the microhand to an operator via an optical fiber bundle to provide the shape and distal information of objects of interest. The use of illuminating fibers along with the optical bundle enables the microhand's operation even in light-deficient environments. Such visual information informs the accurate relative location of the device and the status of manipulation to the operator in real time, who will take subsequent actions accordingly with an increased accuracy and efficiency. Embedding the fiber-based optical system inside the manipulator, instead of using an external camera setup for overall system monitoring, greatly reduces the size of the manipulator and helps increase maneuverability, particularly when operating in a space-limited work area. Tests have been conducted to verify the performance of the visually aided microhand to manipulate millimeter-sized objects in real time. Building on the ability of the UCLA microhand to gently handle irregular-shaped objects, this vision-enabled microhand is expected to provide more accurate manipulations and widen the window of applications.**

***Index Terms*—Microactuator, microelectromechanical systems (MEMS), microhand, microrobot, pneumatic actuation.**

I. Introduction

With the advent of microelectromechanical systems (MEMS) technologies, micromanipulators to perform the assigned work on a small target object in a limited confined work space have become a great interest in many fields including biomedical and microassembly. Actuation methods for such micromanipulators include the use of electrostatic force [1], [2], thermal expansion [3], a shape memory alloy [4]–[6], piezoelectricity [7], and pneumatic force [8], [9]. Recently, micro pneumatic balloon actuators with out-of-plane movement capabilities mimicking a human hand (a "microhand") have been introduced for various biological applications [10], [11] and demonstrated successful device operations, including pulling and moving of micrometer- to millimeter-sized objects.

Manuscript received May 2, 2008; revised January 12, 2009. First published February 6, 2009; current version published April 1, 2009.

W. Choi and C.-J. Kim are with the Mechanical and Aerospace Engineering Department, University of California, Los Angeles (UCLA), Los Angeles, CA 90095 USA (e-mail: cw0101@ucla.edu; cjkim@ucla.edu).

M. Akbarian was with Intelligent Optical Systems, Inc. (IOS), Torrance, CA 90505 USA. She is now with Karl Storz Endoscopy-America, Inc., Culver City, CA 90230 USA (e-mail: minooak@yahoo.com).

V. Rubtsov is with Intelligent Optical Systems, Inc. (IOS), Torrance, CA 90505 USA (e-mail: vrubtsov@intopsys.com).

Color versions of one or more of the figures in this paper are available online at http://ieeexplore.ieee.org.

Digital Object Identifier 10.1109/TIE.2009.2014674

The aforementioned micromanipulators of various device sizes and driving mechanisms lack active real-time motion control by the operator unless used in a well-monitored working environment. Associating the micromanipulators with a status monitoring system, instead of blindly operating the manipulators, can greatly increase the accuracy and work performance because the real-time information transferred from the device to the operator enables the operator to find the device's object manipulating status and determine the required subsequent action. Such monitoring systems for micromanipulation generally include visual and force sensing [12]–[20]. However, those sensing systems have their own drawbacks. Most visual feedback systems rely on large external cameras to monitor the object micromanipulation, which is not a proper choice when the work needs to be done in a space-limited environment where such camera setups cannot be accommodated. Force sensing is the key feedback parameter when the force on the object needs to be monitored and well controlled. For example, Kusuda *et al.* [21] employed a feedback capability by using a fluid-resistive bending sensor to their PDMS-based microfinger device that is millimeters in size to estimate the bending status of microfingers. However, the force sensing alone cannot provide the shape and distal information of the object of interest, still calling for an external camera to monitor the overall manipulator operations.

In this paper, integration of the microhand created by the MEMS technologies and the conventional visual system designed for endoscopic inspection purposes is presented for accurate small-object manipulation. Equipped with an imaging optical fiber bundle along with illuminating fibers inside, this "seeing microhand" allows operators to receive real-time visual information directly from its "palm" without using external camera setups. Furthermore, the microfabrication and the packaging procedure have been modified so that the pressurized air is supplied to the device backside. The new package does not obstruct the microhand's motion, increasing the degree of freedom of the device over the previously introduced microhand [10], [22], which had the air supplied to the frontside.

II. Microhand Designs With Internal Visual System

A. Pneumatic Actuation of Microhand

Fig. 1 shows the working principle of the balloon-based microjoint system inducing an out-of-plane motion [23], [24]. A flexible balloon structure is placed between two separate rigid blocks, as shown in Fig. 1(a). When compressed air is applied to inflate the balloon, the tension pulls the blocks together to

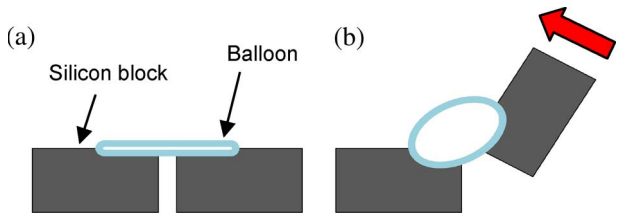

Fig. 1. Schematic illustration of the balloon actuator. (a) Balloon connects two silicon blocks. (b) When the balloon inflates with compressed air, the attached blocks make a relative out-of-plane motion against each other due to the tension of the balloon.

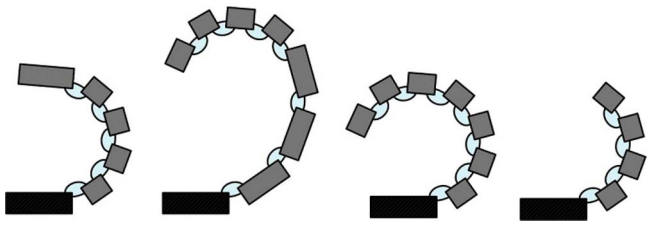

Fig. 2. Various finger curling shapes are determined by the number of joints and the varying lengths of phalanges.

make a relative out-of-plane motion of the blocks, as shown in Fig. 1(b). The angle and the force of the blocks' motion are determined by the pressure of air introduced into the balloon, as well as the geometric dimensions of the balloon and the blocks [22]. When the air is removed from the balloon, the pulling force is removed, and the two blocks return back to the initial position. Here, the balloon works as an active joint to generate a motion.

This balloon joint mechanism was implemented to monolithically construct (i.e., no bonding) a multijoint microfinger by integrating several silicon microfabrication techniques into one continuous process flow [24]. By arranging the microfingers axially and adding the pneumatic paths along with the packaging, a human-handlike micromanipulator has recently been reported by a UCLA team [10].

The number of balloon joints and the length of each phalange block are important parameters in designing the closing shape of a finger and determining the minimum size of objects that a microhand can handle, as shown in Fig. 2. In this paper, a microhand with four fingers, each with seven phalanges and six interconnecting balloons to have a full closure (i.e., fingers curl to form a ball shape), is used, as shown in Fig. 3. The design is based on the data that each joint makes $\sim 35^\circ$ angle at 240 kPa obtained from preliminary tests of equivalent fingers. Each silicon phalange is 600 μm (long) $\times$ 230 μm (wide) $\times$ 120 μm (thick) in size, and each parylene balloon is a 400-μm (long) $\times$ 800-μm (wide) rectangle when fully deflated. Parylene is a biocompatible and chronically stable [25], [26] sealing material featuring a very uniform coating, making it an excellent choice for the balloon material. Each finger is 4 mm long and 800 μm wide. At the "palm" of the four-fingered microhand is a through hole (1.5-mm diameter) where an optical fiber system will be inserted later during the device packaging. The minimum object handling size of the microhand is determined by the gap between the opposing fingertips. The

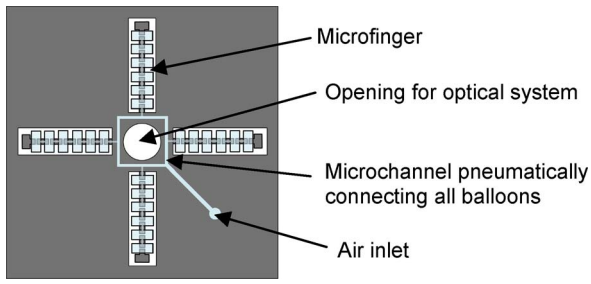

Fig. 3. Four-finger microhand design with a 1.5-mm opening in the "palm." Each finger is 4 mm in length, and the hand forms a fist of 5 mm in diameter at 240 kPa. The distance between the opposing fingers at the anchors is 2.6 mm, and all the balloons are pneumatically connected by microchannels and to the air inlet.

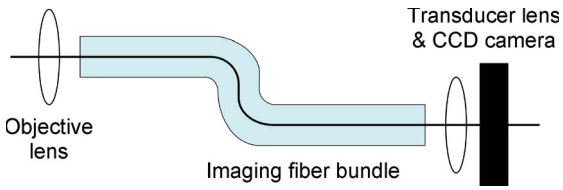

Fig. 4. Schematic of optical system used in this paper. The system consists of the following: 1) an objective lens; 2) an imaging bundle; and 3) a bundle-camera transducer lens and CCD camera.

microhand for this paper is designed to handle and grab objects that are 600 μm to millimeters in size. For even smaller object manipulations, the microhand designs could be changed for their specific applications.

B. Embedded Optical System

1) Imaging System: Incorporating a visual system into the UCLA Microhand is the main goal of this study. A custom-designed optical circuit, as shown in Fig. 4, is used for this study due to the lack of configurability available in optical fibers and lens in commercially available fiber-based endoscopes. The optical circuit mainly consists of three parts: an objective lens, a multifiber imaging bundle, and an imaging bundle-camera transducer lens attached to the charge-coupled device (CCD) camera. The objective lens transmits the image of the target object to the fiber bundle. Considering the diameter of the lens, the working distance range, and field of view (FOV), an objective lens (from Fujikura, Tokyo, Japan) that has 370-μm diameter and 50° FOV to view a 2-mm object from approximately 2-mm distance was chosen. This objective lens has a focus range between 3 and 20 mm. The multifiber imaging bundle transmits the image from the objective lens to the camera through the transducer lens. The imaging bundle used here is the FIGH-06-300S model with 270-μm image circle diameter having 6000 pixels (from Fujikura, Tokyo, Japan) with the resolution of 3.5 μm. The objective lens is attached to the front of the imaging fiber bundle in a designated housing, resulting in an overall housing outer diameter of 550 μm. A 20$\times$ transducer lens (Omex Technologies, IL, USA) is mounted on the CCD camera (DFK 21AF from Imaging Source, NC, USA) and is connected to the imaging bundle housing.

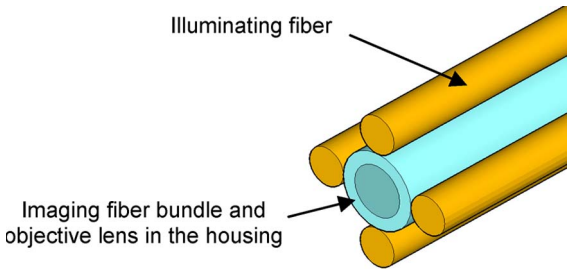

Fig. 5. Arrangement of illuminating fibers and the imaging fiber bundle sealed with the objective lens in the housing. Four illuminating fibers (250 μm in diameter each) are surrounding the imaging fiber housed with the lens with 550-μm overall diameter.

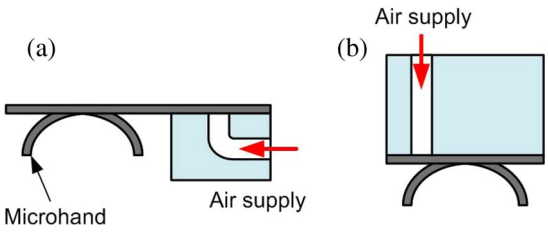

Fig. 6. (a) Air inlet in the frontside of the microhand chip. Previous microhands [10], [22] had the air inlet in the frontside, limiting the operation of the microhand due to the thick packaging attached in the same direction as the microhand's finger motion. (b) Newly developed microhand with the air inlet located in the back of the microhand chip. Because the packaging is attached in the back, the microhand can move and be operated without any obstruction by the packaging.

2) Illumination: For a seeing microhand to work successfully, proper illumination is required along with the imaging system. For this purpose, four plastic fibers (PGS-FB250 model from Moritex, CA, USA) with 250-μm diameter including core and cladding are used for illumination with a white LED at 107 lm (XR-E model from CREE, NC, USA) attached on one end as a light source. The four illuminating fibers and the imaging fiber bundle with the objective lens attached in the front are arranged as in Fig. 5 and are inserted into the plastic cube that will be later bonded to the microhand device.

C. Packaging

Previously introduced microhands [10], [22] had their air inlet on the frontside for structural simplicity, as shown in Fig. 6(a). However, this approach increases the overall size of the microhand system and limits the operation of the microhand because the thick packaging cube attached to the frontside of the microhand chip obstructs the motion of the system when the target object lies on a flat surface. To solve this problem and keep the size small, the air inlet needs to be made from the backside. By having the air inlet in the back, all the packaging parts can be sent to the backside of the micromachined silicon chip [as shown in Fig. 6(b)] so that they do not interfere with the motion of the microhand during the operation. This new version will provide a higher degree-of-freedom operation than the previous microhands.

The device assembly for this study is shown in Fig. 7 for a complete microhand with the optical system. After a microhand

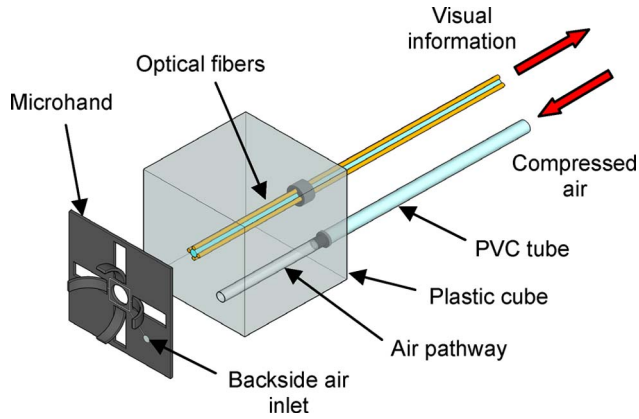

Fig. 7. Illustration of the packaging scheme. Plastic cube with holes for an air pathway and optical fibers is bonded to the back of the microhand chip. The optical fiber bundle is exposed to the front side through the palm opening after packaging. The air pathway is aligned to meet the air inlet at the backside of the microhand chip.

device is made after a series of microfabrication steps that will be revisited in detail in the next section, it is bonded to a plastic cube that is 1 cm a side. The cube has holes for an air pathway and for optical fibers arranged as in Fig. 5. The microhand and the cube should be aligned accurately so that the holes for optical fibers in the plastic cube lie within the palm opening of the microhand, and the air pathway is located exactly on the backside air inlet of the microhand chip. After the bonding, the optical fibers are inserted into the hole in the cube and sealed, and a polyvinyl chloride (PVC) tube is connected to the air pathway by a miniature tube fitting.

III. Fabrication

Fig. 8 shows the fabrication process of the microhand devices. A 150-μm-thick 4-in Si wafer with first (2000-Å) and second (600-Å) thermal oxide layers is patterned and anisotropically etched by deep reactive ion etching (DRIE) to form backside trenches [step (a)]. The second oxide layer under the backside trench surfaces is selectively removed by reactive ion etching, not seriously attacking the oxide on the trench sidewalls. Fabrication details of step (a) are described in [10] and [22]. As mentioned in the previous section, making the air inlet on the backside is the main challenge of this fabrication. For that purpose, more directional etching using DRIE is done on two selective trenches that will be later used for the air-inlet hole and the opening for optical fibers. These trenches are marked with arrows in step (b). In order to perform additional etching only on the selective trenches, all the other trenches that do not require more etching are filled with photoresist and cured to avoid the attack during the DRIE process.

After processing the backside, the topside oxide layers (first and second) are patterned to create the 6-μm $\times$ 6-μm grid holes, through which the subsequent XeF_2 etching is performed to make molds for balloons, followed by conformal parylene deposition. Details of this balloon formation process are explained in [10] and [22]. Step (c) in Fig. 8 shows the shape

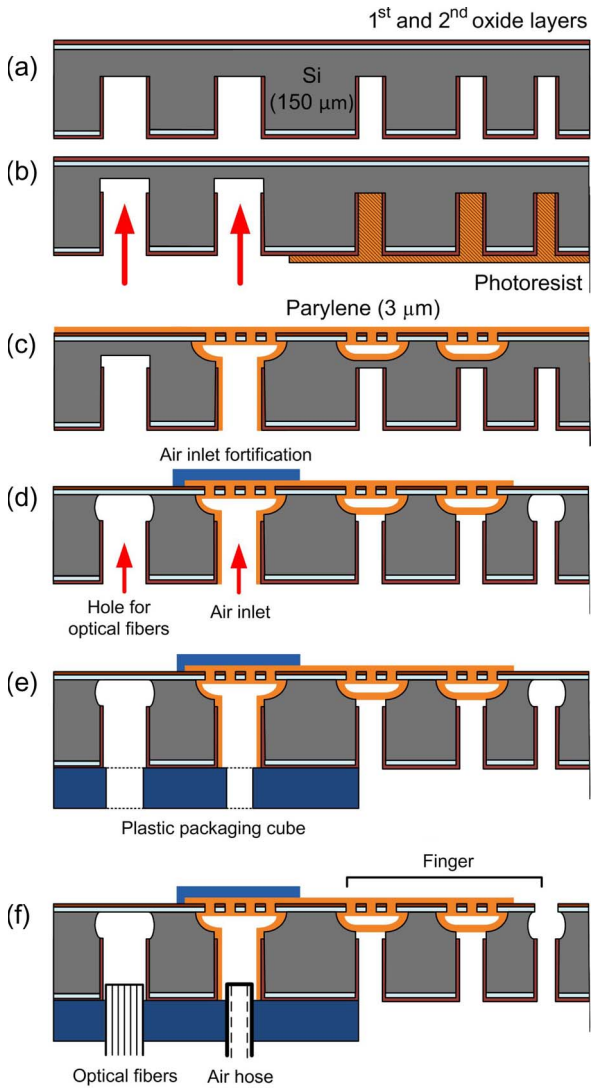

Fig. 8. Fabrication process of the microhand with internal visual system, focusing on the steps modified and added for the internal visual system from the regular microhand fabrication reported in [10] and [22]. (a) Si wafer that is 150-μm thick with oxide layers is patterned and anisotropically etched to form backside trenches, with the oxide layer being selectively removed from the trench surfaces. (b) To make an air inlet and the hole for optical fibers from the backside, additional anisotropic etching by DRIE on selective trenches is performed, with all the other trenches being protected by photoresist. (c) Balloons and microchannels are formed by conformal parylene deposition on the mold etched by the XeF_2 process. (d) Parylene layer is patterned, and the finger is defined by XeF_2. At this stage, the hole for optical fibers is cleared. Epoxy glue is applied on the air-inlet hole to prevent a potential leakage, and the fabricated microhand chips are diced individually. (e) Plastic packaging cube is made and bonded to the fabricated microhand chip. (f) Optical fibers and the air hose are connected via the openings through the plastic cube. Upon applying compressed air, the topside oxide layers are ripped to free the fingers completely.

of the top cavities after 3-μm-thick parylene is coated to form the balloons and microchannels. The second cavity from the left whose backside trench underwent the additional directional etching in the previous step makes a through hole after the XeF_2 etching, while all other cavities are still bottomed with remaining silicon. This through hole will be later used for the backside air inlet.

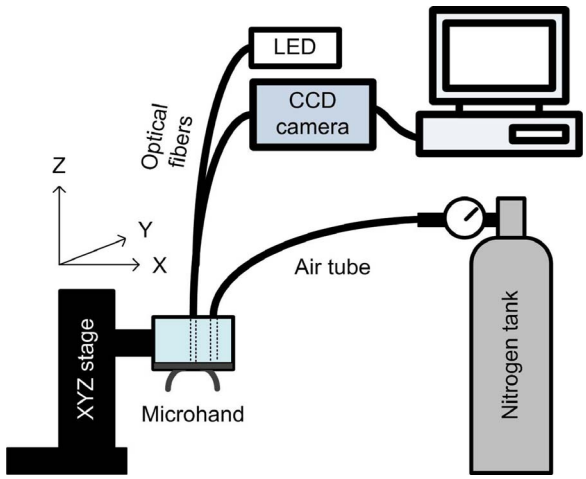

Fig. 9. Schematic of the experimental setup. A pressure-regulator-controlled nitrogen tank and CCD camera are connected to the microhand package by a PVC tube and optical fibers, respectively. Real-time images sent from the palm of the microhand are transferred via optical fibers to the CCD camera that shows the images to an operator. The microhand is held by an XYZ stage that controls the movement.

A following lithography step patterns the deposited parylene layer to allow the release of the fingers during the subsequent "backside" XeF_2 etching [step (d)]. This backside XeF_2 etching step not only removes the remaining silicon in the trenches to free the fingers but also clears the hole for the optical fiber unit. After the finger-releasing step, the parylene membrane on top of the air-inlet hole is fortified with an epoxy-based glue. The fortification prevents possible air leakage during the device operations, considering the imperfect adhesion between the parylene and the silicon wall around the air inlet. Each microhand chip is then diced from the wafer.

A plastic packaging cube is built by a 3-D printing method and epoxy-glued to the diced microhand chip [step (e)]. As the last step [step (f)], the optical fibers and the air hose are inserted through the openings of the plastic cubes. By applying 200–250 kPa of initial pressure, the oxide layer that holds the fingers in place is torn off, and the fingers are now free to move.

IV. Experiment With the Microhand

Fig. 9 shows the schematic view of the test setup for the assembled microhand device. The tube attached to the packaged microhand device is connected on the other end to a nitrogen tank with a pressure regulator where the microhand's finger motion is controlled. The imaging fiber bundle is connected to a CCD camera that transfers the images to a computer screen in real time so that the operators can perceive visual information from the palm of the microhand, while the illuminating fibers are attached to a white LED to enlighten the workspace. The microhand itself is fixed to an XYZ stage to make required movements or location change.

As a preliminary test, the motion of a single 4-mm-long finger is monitored to find out the relationship between the

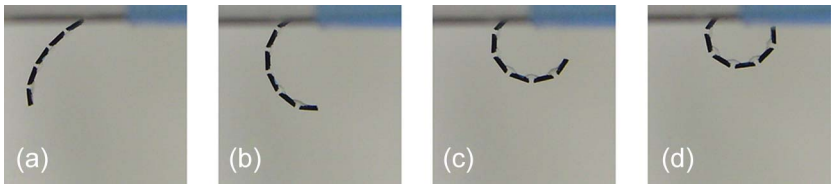

Fig. 10. Side view of a single finger that is 4 mm in length, when (a) no pressure is applied, (b) 140 kPa, (c) 280 kPa, and (d) 410 kPa is applied (0, 20, 40, and 60 lbf/in^2 equivalent, respectively.

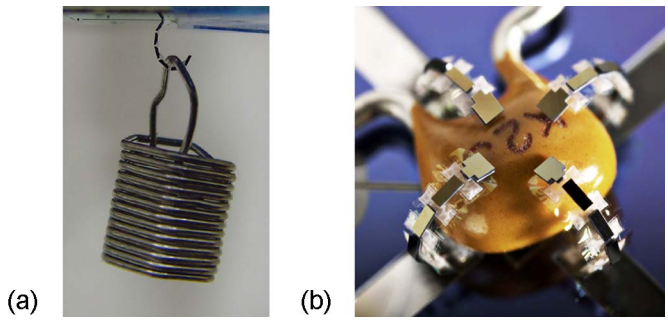

Fig. 11. Photographs of the microhand devices under load testing and size demonstration. (a) Single finger holding a 0.2 g of weight at 760 kPa. (b) Microhand capturing an electric capacitor at 240 kPa making a full closure with 5-mm fist diameter. The microhand is facing up with the capacitor sitting on the "palm" for demonstration purposes only. In the actual case of picking up an object, the microhand faces down, and the object rests against the curled microfingers, ensuring the gap between the grabbed object and the embedded visual system. The microhand photograph has been taken by Jeffrey@intouchliving.com.

applied pressure and the curling pattern of the finger. The sequential figures in Fig. 10 show the curling of the finger at applied pressures of 0, 140, 280, and 410 kPa (0, 20, 40, and 60 lbf/in^2 equivalent, respectively) from left to right. Because of the residual stress in the deposited parylene, the finger is curled up upon fabrication to a certain degree, even with no applied pressure, as shown in Fig. 10(a). Fig. 11(a) shows that a single finger can lift and hold a 0.2-g mass (equivalent to about 2 mN) with an actuation pressure of 760 kPa. A four-fingered microhand, with each finger being 4 mm in length, is shown in Fig. 11(b) holding an electric capacitor. All the parylene microchannels and balloons are pneumatically connected together, sharing the same air supply from the air inlet. Consequently, all the balloons show the same bulging shape, resulting in the same curling pattern of all four fingers. A 240-kPa pressure is applied for full closure of the fingers showing the resultant "fist" diameter of 5 mm as designed, considering the space between the anchors of the fingers at the palm occupied by the optical fibers.

Various objects of different shapes and sizes, such as a piece of plastic tube, a wire, a resistor, and glass pieces, are used for the experiment to demonstrate the microhand's maneuverability with the visual aid. The images transferred from the palm of the microhand are observed and recorded during the experiment. Fig. 12 shows the experiment using a plastic tube piece that is about 3 mm in diameter and 2.5 mm in length. As the tube piece approaches the microhand, as shown in Fig. 12(a) and (b), the image of the object on the screen is magnified. While the microhand grabs the object and the work stage is lowered, as shown in Fig. 12(a) and (b), the image of the object gets even slightly more magnified because the fingers pull the object slightly upward and toward the optical system at the palm of the microhand [Fig. 12(c-1) and (d-1)]. By observing the image on the screen, operators can determine the shape of the object, obtain the distal information between the microhand and the object, and find out whether the microhand successfully grabs the object or not while applying pressure for finger operations.

Another experiment conducted is to sort electric resistors with identical shapes but different number codes printed on them. The microhand translates horizontally at a height of 25–30 mm to locate a resistor of interest, and it picks it up only by visual information sent by the microhand's optical system this time. That is, the operator controls the stage with the attached microhand and confirms that the microhand is located right above the resistor. To have a clear reading of the number written on the resistor, the microhand setup is then lowered so that the distance between the objective lens and the resistor lies within the focus range of the objective lens (3–20 mm). Lighting from the LED source is guided through the four illuminating fibers to ensure clear reading of the numbers in the low-light environment. Once the number is confirmed, the microhand is lowered down further by the operator to pick up the resistor solely relying on the real-time visual image sent by the optical system, as shown in Fig. 13(a), (a-1), (b), and (b-1). After being picked up, the resistor is transported and dropped onto a designated sorting well [Fig. 13(c) and (c-1)]. The releasing of the grabbed resistor is done by releasing the compressed air from the microhand to open the microfingers so that the resistor falls free into the well. Instantaneous releasing of the resistor was achieved using a pressure-relieving setup (from Mead, USA) attached to the pressure regulator.

V. Conclusion

With real-time status monitoring capabilities, micromanipulators can have important advantages in their controls. This paper has presented a seeing microhand device equipped with an internal visual system that is designed for conventional endoscopic applications and successfully demonstrated various tests of object manipulation. Building on the existing UCLA microhand that is capable of gently manipulating irregular objects, this seeing microhand has further been empowered by the self-illuminated internal visual information, facilitating the operation in a confined space that is deficient of light. The new seeing microhand poses as a promising

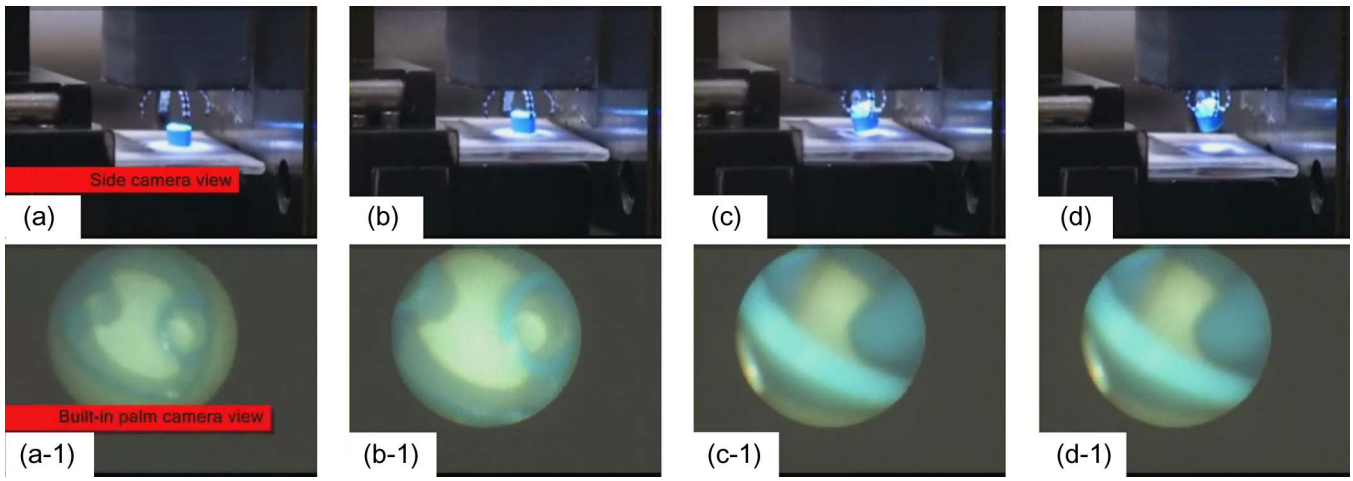

Fig. 12. Microhand with visual system picking up objects. A plastic tube with 3-mm diameter is sliced and used for this experiment. (a) Target object is placed on a stage that can move in vertical direction, (b) the stage is moving upward to near the tube to the microhand, (c) the microhand grabs the tube, and (d) the stage is removed, with the tube being held by the microhand. (a-1), (b-1), (c-1), and (d-1) are the images transferred from the optical unit from the microhand showing the target object, synchronized with (a), (b), (c), and (d), respectively.

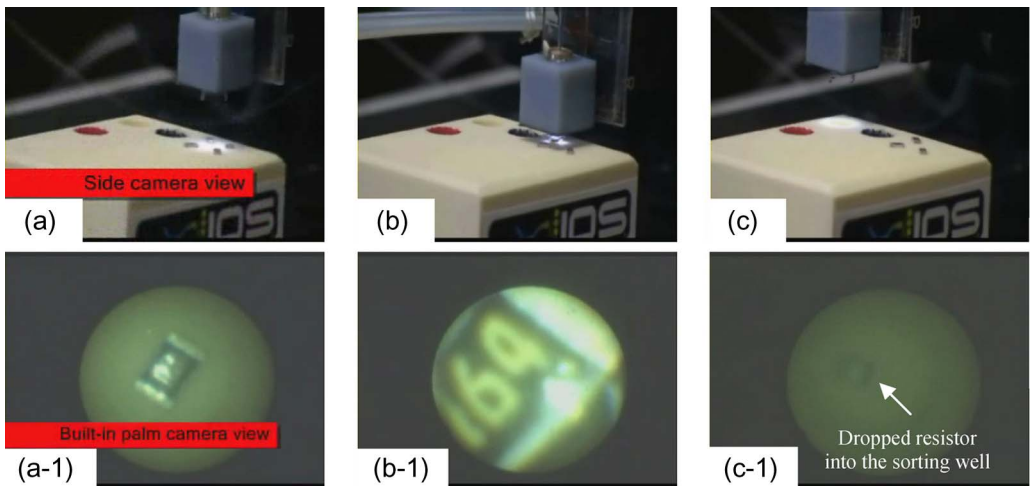

Fig. 13. Operation demonstration with a completed system. Microhand with visual system is sorting electric resistors by reading the numbers written on them. The microhand moves by the attached stage and (a) stops above the resistor of interest, (b) comes down to grab the resistor, and (c) picks up, transfers, and drops the resistor to a designated sorting well. (a-1), (b-1), and (c-1) are the images transferred from the optical unit from the microhand showing the resistor, synchronized with (a), (b), and (c), respectively.

tool for biomedical and industrial applications, including the following:

1) microrobotics for biomedical research and operations;
2) micromanufacturing and microassembly where workspace is limited and has poor visibility or where precise positioning of parts is required;
3) microsurgery with a minimal invasive opening whose operation requires delicate force control and real-time monitoring of the organ in surgery;
4) inspection of a hard-to-reach area that requires the use of endoscopic tools with grippers to perform additional local tasks.

REFERENCES

[1] C.-J. Kim, A. P. Pisano, and R. S. Muller, "Silicon-processed overhanging microgripper," *J. Microelectromech. Syst.*, vol. 1, no. 1, pp. 31–36, Mar. 1992.

[2] B. E. Volland, H. Heerlein, and I. W. Rangelow, "Electrostatically driven microgripper," *Microelectron. Eng.*, vol. 61/62, pp. 1015–1023, Jul. 2002.

[3] W. H. Chu and M. Mehregany, "Microfabricated tweezers with a large gripping force and a large range of motion," in *Proc. Solid-State Sens. Actuators Workshop*, Hilton Head Island, SC, Jun. 1994, pp. 100–107.

[4] P. Krulevitch, A. P. Lee, P. B. Ramsey, J. C. Trevino, J. Hamilton, and M. A. Northrup, "Thin film shape memory alloy microactuators," *J. Microelectromech. Syst.*, vol. 5, no. 4, pp. 270–282, Dec. 1996.

[5] C. S. Pan and W. Hsu, "An electro-thermally and laterally driven polysilicon microactuator," *J. Micromech. Microeng.*, vol. 7, no. 1, pp. 7–13, Mar. 1997.

[6] M. Kohl, E. Just, W. Pfleging, and S. Miyazaki, "SMA microgripper with integrated antagonism," *Sens. Actuators A, Phys.*, vol. 83, no. 1, pp. 208–213, May 2000.

[7] M. C. Carrozza, A. Menciassi, G. Tiezzi, and P. Dario, "The development of a LIGA-microfabricated gripper for micromanipulation tasks," *J. Micromech. Microeng.*, vol. 8, no. 2, pp. 141–143, Jun. 1998.

[8] S. Butefisch, V. Seidemann, and S. Buttgenbach, "Novel micro-pneumatic actuator for MEMS," *Sens. Actuators A, Phys.*, vol. 97/98, pp. 638–645, Jan. 2002.

[9] J. Ok, Y.-W. Lu, and C.-J. Kim, "Pneumatically driven microcage for microbe manipulation in a biological liquid environment," *J. Microelectromech. Syst.*, vol. 15, no. 6, pp. 1499–1505, Dec. 2006.

[10] Y.-W. Lu and C.-J. Kim, "Microhand for biological applications," *Appl. Phys. Lett.*, vol. 89, no. 16, p. 164 101, Oct. 2006.

[11] S. Konishi, M. Nokata, O. C. Jeong, S. Kusuda, T. Sakakibara, M. Kuwayama, and H. Tsutsumi, "Pneumatic micro hand and

miniaturized parallel link robot for micro manipulation robot system," in *Proc. IEEE Int. Conf. Robot. Autom.*, Orlando, FL, May 2006, pp. 1036–1041.

[12] H. Yamamoto and T. Sano, "Study of micromanipulation using stereoscopic microscope," *IEEE Trans. Instrum. Meas.*, vol. 51, no. 2, pp. 182–187, Apr. 2002.

[13] D. H. Kim, K. Kim, K. Y. Kim, and S. M. Cha, "Dexterous teleoperation for micro parts handling based on haptic/visual interface," in *Proc. IEEE Int. Symp. Micromechatron. Human Sci.*, Nagoya, Japan, Sep. 2001, pp. 211–217.

[14] L. D. Wang, J. K. Mills, and W. L. Cleghorn, "Automatic microassembly using visual servo control," *IEEE Trans. Electron. Packag. Manuf.*, vol. 31, no. 4, pp. 316–325, Oct. 2008.

[15] F. Beyeler, A. Neild, S. Oberti, D. J. Bell, Y. Sun, J. Dual, and B. J. Nelson, "Monolithically fabricated microgripper with integrated force sensor for manipulating microobjects and biological cells aligned in an ultrasonic field," *J. Microelectromech. Syst.*, vol. 16, no. 1, pp. 7–15, Feb. 2007.

[16] Z. Lu, P. C. Y. Chen, J. Nam, R. W. Ge, and W. Lin, "A micromanipulation system with dynamic force-feedback for automatic batch microinjection," *J. Micromech. Microeng.*, vol. 17, no. 2, pp. 314–321, Feb. 2007.

[17] T. Chu Duc, G. K. Lau, J. F. Creemer, and P. M. Sarro, "Electrothermal microgripper with large jaw displacement and integrated force sensors," in *Proc. IEEE Conf. Micro Electro Mech. Syst.*, Tucson, AZ, Jan. 2008, pp. 519–522.

[18] T. Slama, A. Trevisani, D. Aubry, R. Oboe, and F. Kratz, "Experimental analysis of an Internet-based bilateral teleoperation system with motion and force scaling using a model predictive controller," *IEEE Trans. Ind. Electron.*, vol. 55, no. 9, pp. 3290–3299, Sep. 2008.

[19] N. Ando, P. Korondi, and H. Hashimoto, "Networked telemicromanipulation systems 'Haptic Loupe'," *IEEE Trans. Ind. Electron.*, vol. 51, no. 6, pp. 1259–1271, Dec. 2004.

[20] Y. Matsumoto, S. Katsura, and K. Ohnishi, "Dexterous manipulation in constrained bilateral teleoperation using controlled supporting point," *IEEE Trans. Ind. Electron.*, vol. 54, no. 2, pp. 1113–1121, Apr. 2007.

[21] S. Kusuda, S. Sawano, and S. Konishi, "Fluid-resistive bending sensor having perfect compatibility with flexible pneumatic balloon actuator," in *Proc. IEEE Conf. Micro Electro Mech. Syst.*, Kobe, Japan, Jan. 2007, pp. 615–618.

[22] Y.-W. Lu, "Microcage and microhand for object manipulation in microscale," Ph.D. dissertation, Mech. Aerosp. Eng. Dept., Univ. California, Los Angeles, CA, 2004.

[23] F. Kawai, P. Cusin, and S. Konishi, "Thin flexible end-effector using pneumatic balloon actuator," in *Proc. IEEE Conf. Micro Electro Mech. Syst.*, Miyazaki, Japan, Jan. 2000, pp. 391–396.

[24] Y.-W. Lu and C.-J. Kim, "Characterization of balloon-jointed microfingers," in *Proc. MEMS, ASME IMECE*, Washington, DC, Nov. 2003, vol. 2003-41326, pp. 311–316.

[25] G. Y. Yang, G. Johnson, W. C. Tang, and J. H. Keyak, "Parylene-based strain sensors for bone," *IEEE Sensors J.*, vol. 7, no. 12, pp. 1693–1697, Dec. 2007.

[26] P. J. Chen, D. C. Rodger, R. Agrawal, S. Saati, E. Meng, R. Varma, M. S. Humayun, and Y. C. Tai, "Implantable micromechanical parylene-based pressure sensors for unpowered intraocular pressure sensing," *J. Micromech. Microeng.*, vol. 17, no. 10, pp. 1931–1938, Oct. 2007.

Wook Choi received the B.S. degree in mechanical engineering from Kyungpook National University, Daegu, Korea, in 2002, and the M.S. degree from the Mechanical and Aerospace Engineering Department, University of California, Los Angeles (UCLA), Los Angeles, in 2005, where he is currently working toward the Ph.D. degree.

His research interests include the design and fabrication of pneumatic and electrostatic microdevices for various applications using MEMS technologies.

Dr. Choi is currently a member of the Korean–American Scientists and Engineers Association. He was a recipient of scholarships from the Korea Science and Engineering Foundation.

Minoo Akbarian received the B.S. degree in electrical engineering and control systems from the University of Tehran, Tehran, Iran, in 1998, and the M.S. degree in electrical engineering from the University of Southern California, Los Angeles, in 2000.

After graduation, she was with Intelligent Optical Systems, Inc. (IOS), Torrance, CA, where she was a Research Engineer and worked on many research projects in the area of electro-optical systems and sensors. Since December 2008, she has been with Karl Storz Endoscopy-America, Inc., Culver City, CA, as a Product Manager for KARL STORZ OR1^{TM} operating rooms.

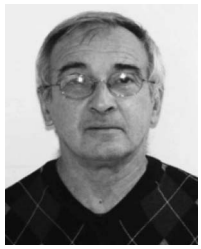

Vladimir Rubtsov received the Ph.D. degree in applied physics from the Nondestructive Control Research Institute, Kharkov, Ukraine (formerly U.S.S.R.).

He has been with Intelligent Optical Systems, Inc. (IOS), Torrance, CA, as a Senior Scientist since 2000. His expertise is in nondestructive testing, fiber-optic and LED illumination, endoscopy, optical sensors, and fiber laser development. He has developed devices for the U.S. Navy, the U.S. Army, the National Institutes of Health, the National Science Foundation, DARPA, Homeland Security, and NASA. He has conducted more than 50 projects and is the holder of four U.S. patents and seven Russian patents. His research career in the U.S. includes positions such as Staff Researcher with the Surgery Department of UCLA Medical Center Research Laboratory (Los Angeles, CA, 1992–2001), and Fiber Optic Program Manager with FarLight Corporation (Torrance, CA, 1996–2000).

Chang-Jin "CJ" Kim (S'89–M'91) received the Ph.D. degree in mechanical engineering from the University of California, Berkeley, in 1991.

He has been a Faculty Member with the Mechanical and Aerospace Engineering Department of the University of California, Los Angeles (UCLA) since 1993 and directs the Micro and Nano Manufacturing Laboratory. His research interests are in MEMS and nanotechnology, including design and fabrication of micro-/nanostructures, actuators, and systems, with a focus on the use of surface.

Dr. Kim is currently the Chair of the Devices and Systems Committee of the ASME Nanotechnology Institute and a Member of the Editorial Board of the JOURNAL OF MICROELECTROMECHANICAL SYSTEMS, of the Editorial Advisory Board for the *IEEJ Transactions on Electrical and Electronic Engineering*, and of the National Academies Panel on Benchmarking the Research Competitiveness of the U.S. in Mechanical Engineering. He is the recipient of the TRW Outstanding Young Teacher Award, the NSF CAREER Award, the ALA Achievement Award, and the Samueli Outstanding Teacher Award. He has served on numerous professional and governmental committees and panels on MEMS and nanotechnology.